THE BELL SYSTEM
TECHNICAL JOURNAL

VOLUME XXXVI NOVEMBER 1957 NUMBER 6

A New Storage Element Suitable for Large-Sized Memory Arrays—The Twistor

By ANDREW H. BOBECK

Three methods have been developed for storing information in a coincident-current manner on magnetic wire. The resulting memory cells have been collectively named the "twistor". Two of these methods utilize the strain sensitivity of magnetic materials and are related to the century old Wertheim or Wiedemann effects; the third utilizes the favorable geometry of a wire.

The effect of an applied torsion on a magnetic wire is to shift the preferred direction of magnetization into a helical path inclined at an angle of 45° with respect to the axis. The coincidence of a circular and a longitudinal magnetic field inserts information into this wire in the form of a polarized helical magnetization. In addition, the magnetic wire itself may be used as a sensing means with a resultant favorable increase in available signal since the lines of flux wrap the magnetic wire many times. Equations concerning the switching performance of a twistor are derived.

An experimental transistor-driven, 320-bit twistor array has been built. The possibility of applying weaving techniques to future arrays makes the twistor approach appear economically attractive.

I. INTRODUCTION

A century ago Wiedemann[1] observed that if a suitable magnetic rod which carries a current is magnetized by an external axial field, a twist

of the rod will result. The effect is a consequence of the resultant helical flux field causing a change in length of the rod in a helical sense. Conversely, it was also observed that a rod under torsion will produce a voltage between its ends when the rod is magnetized (see Fig. 1).

Recently, during an investigation of the magnetic properties of nickel wire, it was observed that a voltage was developed across the ends of a nickel wire as its magnetization state was changed. Both the amplitude and the polarity of the observed signal could be varied by movements of the nickel wire. Most surprising, the amplitude of the observed voltage v_2 of Fig. 2, was many times that which would be expected if a conventional pickup loop were used.

After determining experimentally that the observed voltage was generated solely in the nickel wire and was not a result of air flux coupling the sensing loop (nickel wire plus unavoidable copper return wire), it was concluded that the flux in the nickel wire must follow a helical path. This suggested that torsion was the cause of the observed effect, a conclusion verified experimentally. The direction of the applied twist de-

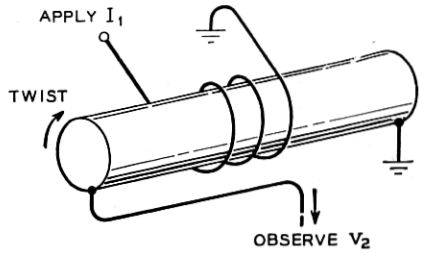

Fig. 1 — Observation of an internally induced voltage v_2 generated by a magnetic wire under torsion.

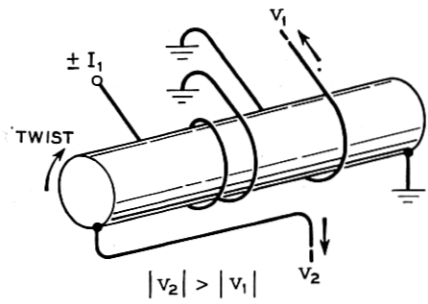

Fig. 2 — Comparison of the internally induced voltage v_2 to the voltage v_1 induced in the pickup loop.

termined the polarity and the amount of the twist determined the magnitude of the observed voltage.

As a consequence of these results, it is possible to build mechanical-to-electrical transducers,[2] transformers with unity turns ratio but possessing a substantial transforming action, and a variety of basic memory cells.

This paper will be concerned with a discussion of the memory cells from both a practical and theoretical viewpoint. It will be shown how these cells can be fabricated into memory arrays. One such configuration consists solely of vertical copper wires and horizontal magnetic wires. Experimental results of the switching behavior of many magnetic materials when operated in the "twisted" manner will be given.

II. A COINCIDENT-CURRENT MEMORY CELL — THE TWISTOR

Consider a wire rigidly held at the far end and subjected to a clockwise torsion applied to the near end. This will result in a stress component of maximum compression[3] at an angle of 45° with respect to the axis of the wire in the right-hand screw sense, and a component of maximum tension following a left-hand screw sense. All magnetic materials are strain sensitive to some degree. This will depend upon both the chemical composition and the mechanical working of the material. For example, if unannealed nickel wire is subjected to a torsion, the preferred direction of magnetization will follow the direction of greatest compression, as would be predicted from the negative magnetostrictive coefficient of nickel. Unannealed nickel wire, then, will have a preferred remanent flux path as shown in Fig. 3.

If the ease of magnetization as measured along the helix is sufficiently lower than that along the axis or circumference, it is possible to insert information into the wire in a manner somewhat analogous to the usual

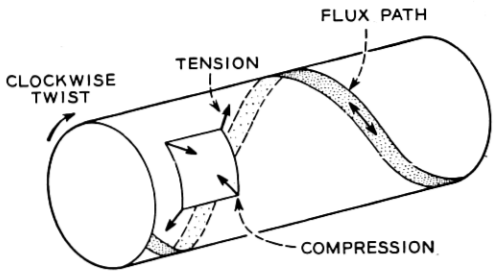

Fig. 3 — Relationship of the mechanical stresses resulting from applied torsion to the preferred magnetic flux path in nickel.

coincident-current method. Consider a current pulse I_1 applied through the nickel wire in such a direction as to enhance the spiraling flux, and a second current pulse I_2 applied by means of an external solenoid (see Fig. 4). Coincidentally, the proper amplitude current pulses will switch the flux state of the wire; either alone will not be sufficient. To sense the state of the stored information it is necessary either to reverse both currents, or to overdrive I_2 in the reverse direction. In an array, the output, in the form of a voltage pulse, would be sensed across the ends of the nickel wire. The solenoid may be replaced by a single copper conductor passing at right angles to the nickel wire. For obvious reasons the memory cell has been named the "twistor". The above method of operation will be referred to as mode A.

Mode B is the use of the magnetic wire as a direct replacement for the conventional coincident-current toroid. Its use here differs only in that the wire itself is used as a sensing winding (refer to Fig. 5). The pulses I_1 and I_2 are equal in value and each alone is chosen to be insufficient to switch the magnetization state of the wire. The coincidence of I_1 and I_2 will, however, result in the writing of a bit of information into the wire. To read, I_1 and I_2 are reversed in polarity and applied coincidently. The output appears as a voltage pulse across the ends of the nickel wire.

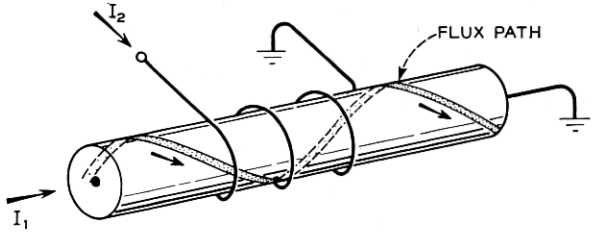

Fig. 4 — Coincident currents for the "write" operation in a twistor operated mode *A*. Wire under torsion.

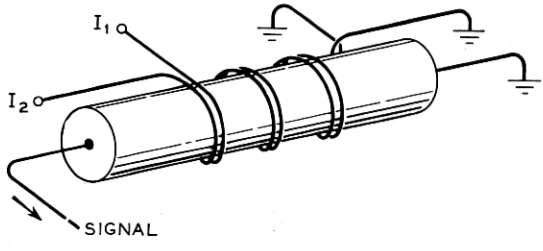

Fig. 5 — For mode *B* the coincidence of I_1 and I_2 is required to exceed the knee of the φ-NI characteristic. Wire under torsion.

The third method of operating the twistor, mode C, is similar in nature to a method proposed by J. A. Baldwin.[4] In this scheme the wire is not twisted, so that neither screw sense is favorable. By the proper application of external current pulses, information will be stored in the wire in the form of a flux path of a right-hand screw sense for a "1", and a left-hand screw sense for a "0". The operation of the cell is indicated in Figure 6. Note that the writing procedure requires a coincidence of currents; the reading procedure does not. The sign of the output voltage indicates the stored information.

Modes A and C are best suited for moderate sized memory arrays since the reading procedure is not a coincident type selection. Thus to gain access to n^2 storage points, an access switch capable of selecting one of n^2 points is required. For large arrays the use of mode B is indicated. It then becomes possible to select one of n^2 points with a $2n$ position access switch. The crossover point (about 10^5 bits) is determined by access circuitry considerations.

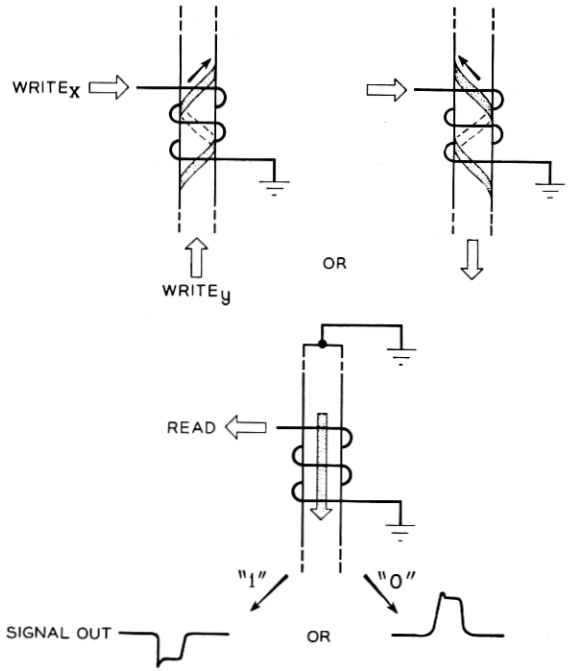

Fig. 6 — Read-write cycle for a twistor operated mode *C*. The wire is not under torsion.

III. ANALYSIS OF THE SWITCHING PROPERTIES OF THE TWISTOR

Section 3.1 will deal with the basic properties of magnetic wire as they pertain to the twistor memory cell. Section 3.2 will be concerned with a composite magnetic wire. The theoretical conclusions will be supported by experimental results wherever possible.

3.1 *Solid Magnetic Wire*

It has been stated above that there is a voltage gain inherent in the operation of the twistor. This voltage gain makes it possible to obtain millivolt signals from wires several mils in diameter. An expression will now be derived relating the axial flux of an *untwisted* wire to the circular flux component of that wire when twisted. Assume that the magnetic wire has been twisted so that the flux spirals at an angle θ (normally $\theta = 45°$) with respect to the axis of the wire. If d and l are the diameter and length of the magnetized region respectively, then, for a complete flux reversal the change in the *circular* flux component is $\varphi_{circ} = l(d/2)(2B_s \sin \theta)$.

Here, φ_{circ} is the flux change that would be observed on a hypothetical pickup wire which passed down the axis of the magnetic wire. The flux change which would be observed by a single pickup loop around the wire, if the magnetic wire were not twisted, is $\varphi_{longitudinal} = \pi d^2 B_s/2$. Therefore, $\varphi_{circ}/\varphi_{long} = 2\ l \sin \theta/\pi\ d$, and for $\theta = 45°$, this expression reduces to

$$\frac{\varphi_{circ}}{\varphi_{long}} = \frac{l/d}{2.22}. \tag{1}$$

Thus, for example, if the storage length on a 3-mil wire is 100 mils, then a 15:1 gain in flux change (or voltage) is obtained.

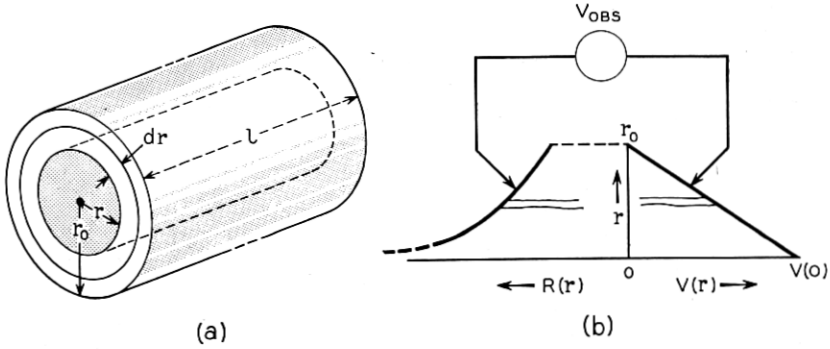

Fig. 7 — (a) Calculation of the observable voltage V_{obs} for a solid magnetic wire. (b) Diagram of induced voltage $V(r)$ and resistance $R(r)$.

The above derivation assumed that the entire circular flux change could be observed externally. Since the magnetic wire must, of necessity, serve as the source of the generated voltage the resultant eddy current flow reduces the *observable* flux change by a factor of three. Consider Fig. 7; assume that the flux reversal takes place in the classical manner and consider the circular component of this flux since it alone contributes to the observable signal. The induced voltage $V(r)$ at any point r is $V(r) = V(0)/(r_0 - r/r_0)$, where r_0 is the radius of the wire and $V(0)$ the voltage at $r = 0$. But $V(r)$, the induced or open-circuit voltage per length of wire l, could only exist if the wire were composed of many concentric tubes of wall thickness dr, each insulated from one another. In a long wire no radial eddy currents can exist. Therefore the wire of length l can be assumed to be faced by a perfect conductor at both of its ends. It remains to calculate the potential between these ends. The resistance of the tube is $R(r) = \rho l/2\pi r\, dr$, where ρ is the resistivity in ohm-cm. The resistance of the wire is given by $R_0 = \rho l/\pi r_0^2$. These resistances form a voltage divider on the *induced* voltage in the tube and the total contribution of all tubes is obtained by integration;

$$\begin{aligned} V_{\text{observed}} &= \int_0^{r_0} V(r) \left(\frac{\rho l/\pi r_0^2}{\rho l/2\pi r dr} \right) \\ &= \int_0^{r_0} V(0) \left(\frac{r_0 - r}{r_0} \right) \frac{2r}{r_0^2}\, dr \\ &= \frac{V(0)}{3}. \end{aligned} \tag{2}$$

Thus, (1) must be modified by (2) with the voltage step-up per memory cell becoming,

$$\frac{V_{\text{obs}}}{V_{\text{long}}} = \frac{l/d}{6.66}. \tag{3}$$

3.11 *Bulk Flux Reversal — Classical Case*

The switching performance of a magnetic wire under transient conditions will now be considered. The speed of magnetization reversal of magnetic materials under pulse conditions is best characterized by s_w, the switching coefficient, usually expressed in oersted-microseconds. It is defined as the reciprocal of the slope of the $1/T_s$ versus H curve where T_s is the time required to reverse the magnetization state and H is the applied magnetic field intensity. Only eddy current losses will be considered.

First, consider the case in which the magnetization is entirely circular. Reversal from one flux remanent state to the other is assumed to occur uniformly in time T_s. Axial eddy currents will flow down the center of the wire and return along the surface. The switching coefficient, s_w, will be obtained by equating the input energy to the dissipated energy. The total energy dissipated per unit length is,

$$\mathcal{E} = T_s \int_0^{r_0} 2\pi r P(r)\, dr, \tag{4}$$

and

$$P(r) = \frac{[E(r)]^2}{\rho}, \tag{5}$$

where $P(r)$ the power density is given by $E(r)$ the voltage gradient squared divided by the resistivity. The average energy per unit volume is therefore

$$\mathcal{E}_{\text{av/cm}^3} = \frac{T_s}{\pi r_0^2} \int_0^{r_0} \frac{\left(V(0)\left(\frac{r_0 - r}{r_0}\right) - \frac{V(0)}{3}\right)^2}{\rho l^2} 2\pi r\, dr = \frac{T_s}{18\rho}\left(\frac{V(0)}{l}\right)^2. \tag{6}$$

Now $V(0) = [(dB/dt)r_0 l]10^{-8}$, so $V(0)/l = (2B_s r_0/T_s)10^{-8}$. Putting this expression into (6) yields

$$\mathcal{E}_{\text{aver/cm}^3} = \frac{2B_s^2 r_0^2}{9\rho T_s} 10^{-16}. \tag{7}$$

The input energy per unit volume is

$$\mathcal{E}/\text{cm}^3 = \frac{(2B_s H \cos\theta_1)\ 10^{-7}}{4\pi}, \tag{8}$$

since $\Delta\bar{B}\cdot\bar{H} = 2B_s H \cos\theta_1$ where θ_1 is the angle between the applied field H and the switching flux. The factor $10^{-7}/4\pi$ is a constant relating the energy in joules to the BH product in gauss-oersteds. By equating (7) and (8), and replacing H by $(H - H_0)$, the desired s_w expression is obtained;

$$s_w = T_s(H - H_0) = \frac{(4\pi B_s r_0^2)\ 10^{-3}}{9\rho \cos\theta_1} \text{ (oe-}\mu\text{sec)}. \tag{9}$$

The substitution of $H - H_0$ for H requires some explanation. The switching curve of $1/T_s$ versus H is not a straight line as would be pre-

dicted from (9) but generally possesses considerable curvature at low drives. Equation (9) satisfactorily predicts the slope of the switching curve in the high drive region, but H_0 must be determined experimentally. In Section 3.12, flux reversal by wall motion is treated as it is a possible switching mechanism at low drives.

The switching coefficient s_w for the case in which the magnetization is purely axial will now be treated. As above, the flux density will change from $-B_s$ to $+B_s$ uniformly in time T_s. The eddy currents, which are circular, result from an induced voltage $V(r)$ where $V(r) = [V(r_0)(r/r_0)^2]$, and $V(r_0)$ is given by $V(r_0) = [(2B_s/T_s)\pi r_0^2]10^{-8}$. Thus, $E(r) = V(r)/2\pi r$, and $E(r) = (B_s r/T_s)10^{-8}$. Following the procedure used above, the internally dissipated energy density is

$$\begin{aligned} \mathcal{E}_{\text{av/cm}^3} &= \frac{T_s}{\pi r_0^2} \int_0^{r_0} \frac{(B_s r 10^{-8}/T_s)^2}{\rho} 2\pi r \, dr, \\ \mathcal{E}_{\text{av/cm}^3} &= \left(\frac{B_s^2 r_0^2}{2T_s \rho}\right) 10^{-16}. \end{aligned} \tag{10}$$

Equating this expression to (8) yields

$$s_w = (H - H_0)T_s = \frac{\pi B_s r_0^2 10^{-3}}{\rho \cos \theta_2}, \tag{11}$$

where θ_2 is defined as the angle between the applied field and the switching flux now assumed axial.

The helical flux vector in a twistor can be resolved into a circular and an axial component. Fortunately, since the dissipated energy is proportional to the eddy current density squared, and the axial and circular current density vectors are perpendicular to each other, it is possible to write

$$\mathcal{E}_{\text{av/cm}^3}(\text{helical}) = \mathcal{E}_{\text{av/cm}^3}(\text{axial}) + \mathcal{E}_{\text{av/cm}^3}(\text{circular}). \tag{12}$$

It follows, for a 45 degree pitch angle, that

$$s_w(\text{helical}) = \frac{s_w(\text{axial}) + s_w(\text{circular})}{2} \tag{13}$$

where the factor "2" is a consequence of the flux density components being smaller by $1/\sqrt{2}$ than their resultant. Substitution of (9) and (11) into (13) gives the desired switching coefficient

$$s_w(\text{helical}) = (H - H_0)T_s = \frac{13\pi}{18} \frac{B_s r_0^2 10^{-3}}{\rho \cos \theta}. \tag{14}$$

The term $\cos\theta$ requires further explanation. The magnetization vector is constrained by energy considerations to align with the easy direction of magnetization. The angle between the applied field and the easy direction of magnetization is called θ. Equation (14) is valid for any direction of applied field. The angles θ_1 and θ_2 used in deriving (9) and (11) respectively are each 45 degrees for the helical pitch angle assumed above.

Equation (14) indicates that for maximum switching speed a material with low saturation flux density and high resistivity is required. The lower limit on s_w will be determined by internal loss mechanisms not treated here. Experimentally, this lower bound is found to be approximately 0.2 oe-μsec.

3.12 *Reversal by Single Wall*

The switching time of a twistor when operating in a memory array under coincident current conditions will depend upon the low-drive switching coefficient. Experimentally, it is observed that the low drive s_w is several times the high-drive value. In this section, following the method of Williams, Shockley, and Kittel,[5] flux reversal by the movement of a single wall will be treated. Only the circular flux case will be considered.

The technique used to obtain s_w is identical to that used in Section 3.1.1 except it is postulated that a single wall concentric to the wire moves either from the wire surface inward, or from the wire axis outward. The result is independent of the direction in which the wall moves. Assume the wall moves from $r = 0$ to $r = r_0$, as indicated in Fig. 8. In-

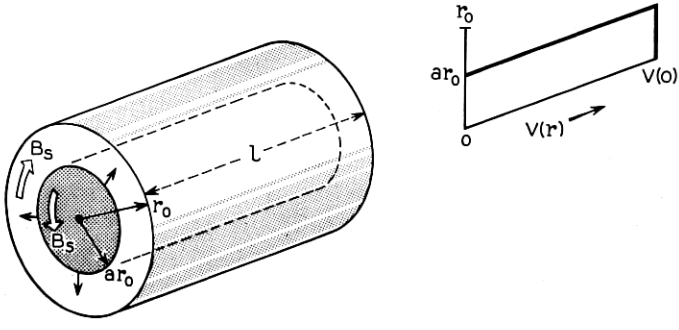

Fig. 8 — Flux reversal by expanding wall instantaneously located at radial position ar_0 moving with velocity v.

stantaneously, the wall is located at ar_0 and is traveling with a velocity v. The induced voltage $V_{oc}(r)$ is,

$$\begin{aligned} V_{oc}(r) &= (2B_s lv)10^{-8} && 0 < r < ar_0 , \\ &= 0 && ar_0 < r < r_0 , \end{aligned} \tag{15}$$

and the observable voltage for a wire of length l is given by

$$\begin{aligned} V_{sc} &= \int_0^{r_0} V_{oc}(r) \frac{\rho l/\pi r_0^2}{\rho l/2\pi r dr} \\ &= \int_0^{ar_0} V_{oc}(r) \frac{2r}{r_0^2} dr \\ &= a^2 V_{oc}(r). \end{aligned}$$

It is clear in the above integration that $V_{oc}(r)$ must be treated as a constant. Using expressions (4) and (5)

$$\frac{\partial \mathcal{E}_{\text{av/cm}^3}}{\partial t} = \frac{1}{\pi r_0^2 \rho} \int_0^{ar_0} \left(\frac{V_{oc}}{l}\right)^2 (1 - a^2)^2 2\pi r dr + \frac{1}{\pi r_0^2 \rho} \int_{ar_0}^{r_0} \left(\frac{V_{oc}}{l}\right)^2 (0 - a^2)^2 2\pi r dr, \tag{16}$$

$$\frac{\partial \mathcal{E}_{\text{av/cm}^3}}{\partial t} = \left(\frac{V_{oc}}{l}\right)^2 \frac{(1 - a^2)a^2}{\rho}.$$

The rate of applying energy is

$$\frac{\partial \mathcal{E}}{\partial t} = \left(\frac{\partial B}{\partial t} \frac{(H - H_c) \cos \theta}{4\pi}\right) 10^{-7}. \tag{17}$$

Once again hysteresis losses are not included. Since $\partial B/\partial t = 2B_s v r_0$, and V_{oc} is given by (15), the equation of (16) and (17) yields,

$$(1 - a^2)a^2 v = \frac{\rho(H - H_c) \cos \theta}{8\pi B_s r_0}.$$

Since $v = (dr/dt) = r_0 (da/dt)$,

$$\int_0^a a^2(1 - a^2)\, da = \frac{\rho(H - H_c) \cos \theta}{8\pi B_s r_0^2} \int_0^t dt,$$

$$\frac{a^3}{3} - \frac{a^5}{5} = \frac{\rho(H - H_c) \cos \theta}{(8\pi B_s r_0^2)10^{-9}} (t + K).$$

When a equals 0, t equals 0, so the constant of integration is zero. When a equals 1, t equals T_s, so

$$s_w = T_s(H - H_c) = \left(\frac{16\pi}{15}\frac{B_s r_0^2}{\rho \cos\theta}\right) 10^{-3}(\text{oe-}\mu\text{sec}) \tag{18}$$

Comparison to the corresponding bulk flux reversal case indicates that the wall motion mechanism is more lossy by a factor of 2.4.

3.2 *The Composite Magnetic Wire*

It is apparent from the switching data of Fig. 9 that for reasonably sized solid wires ($r_0 > 1$ mil) the switching coefficient s_w is unreasonably high. The typical ferrite memory toroid, for example, when used as a memory element has an s_w of 0.6 oersted-microseconds. The only possibility for high speed coincident-current operation for solid magnetic wires is that the material have a high coercive force H_c, a conclusion not consistent with the trend toward transistor driven memory systems.

By the use of a composite wire it should be possible to reduce the eddy current losses and still preserve a reasonable wire diameter. A composite wire, by definition, will consist of a non-magnetic inner wire clad with a magnetic skin. It may be fabricated by a plating or an extruding process.

The solid wire analysis of Section 3.1 is a special case of composite

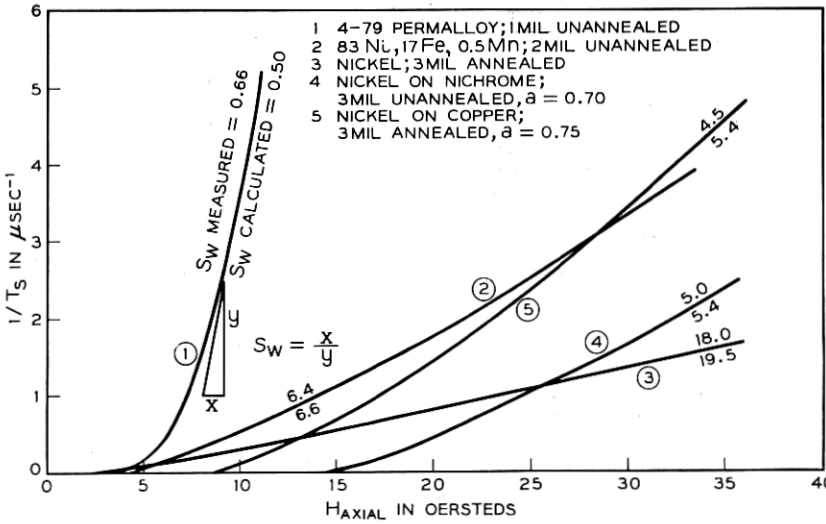

Fig. 9 — Reciprocal of flux reversal time T_S as a function of applied axial drive, H, for solid and composite magnetic wires. Sufficient torsion applied to reach saturation.

wire analysis which is given in Appendix I. Only the results of the composite wire case will be given here. As indicated in Fig. 10, ρ_1 and ρ_2

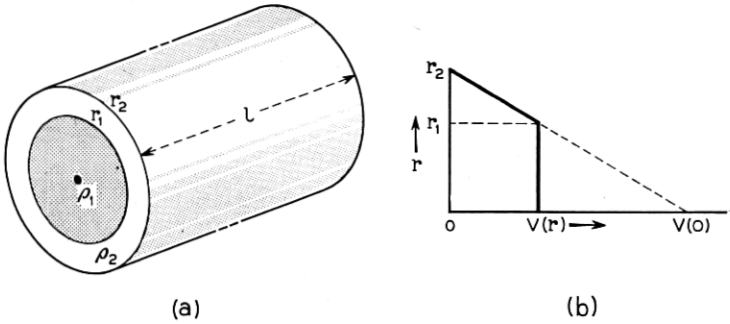

Fig. 10 — (a) Composite wire is composed of non-magnetic core covered by a magnetic skin. (b) A voltage $V(r)$ is induced in the wire during flux reversal.

are the resistivities of the inner (non-magnetic) and outer (magnetic) materials. The inner material is contained within a radius r_1. The overall wire radius is r_2. Defining $a = r_1/r_2$, if V_{obs} is the voltage observed across the ends of the composite wire twistor memory cell, and $V(0)$ is the induced voltage at $r = 0$ for a *solid* magnetic wire of radius r_2, $V_{obs} = bV(0)$, and

$$b = \frac{\frac{\rho_1}{\rho_2}\left(\frac{1}{3} - a^2 + \frac{2}{3}a^3\right) + a^2 - a^3}{\frac{\rho_1}{\rho_2}(1 - a^2) + a^2}. \tag{19}$$

The parameter "b" reduces to $\frac{1}{3}$ for $a = 0$ in agreement with (2) which was derived for the solid wire case. Table I gives "b" for various material and geometry combinations.

TABLE I — THE PARAMETER "b"

ρ_1/ρ_2	a			
	0.9	0.8	0.7	0.0 (Solid Wire)
0	0.100	0.200	0.300	1.000
$\frac{1}{10}$	0.0988	0.194	0.285	.333
$\frac{1}{3}$	0.0963	0.184	0.259	.333
1	0.0903	0.163	0.219	.333
3	0.0790	0.135	0.180	.333
10	0.0643	0.112	0.155	.333
∞	0.0491	0.0963	0.141	.333

TABLE II — THE PARAMETER "C_{circ}"

ρ_1/ρ_2	a			
	0.9	0.8	0.7	0.0 (Solid Wire)
0	0.0858	0.353	0.820	1.396
$\frac{1}{10}$	0.0847	0.339	0.763	1.396
$\frac{1}{3}$	0.0842	0.311	0.657	1.396
1	0.0737	0.256	0.498	1.396
3	0.0595	0.159	0.341	1.396
10	0.0286	0.124	0.243	1.396
∞	0.0209	0.0833	0.186	1.396

The switching coefficient, s_w, for circular flux reversal, is derived as

$$s_w = \frac{(8\pi B_s r_2^2)10^{-3}}{\rho_2(1-a^2)\cos\theta}\left\{a^2\left[(1-a-b)^2\frac{\rho_2}{\rho_1} - (1-b)^2 + \frac{4a(1-b)}{3} - \frac{a^2}{2}\right] + (1-b)^2 - \frac{4(1-b)}{3} + \frac{1}{2}\right\}, \tag{20}$$

or

$$s_w = C_{\text{circ}}\frac{(B_s r_2^2)10^{-3}}{\rho_2\cos\theta}\ (\text{oe-}\mu sec). \tag{21}$$

Table II gives C_{circ} as a function of a and ρ_1/ρ_2.

The switching coefficient s_w for axial flux reversal is derived as

$$s_w = \left(\frac{\pi B_s r_2^2 10^{-3}}{\rho_2\cos\theta}\right)\left(\frac{1-4a^2+a^4(3-4\ln a)}{1-a^2}\right) \tag{22}$$

$$= C_{\text{axial}}\left(\frac{B_s r_2^2 10^{-3}}{\rho_2\cos\theta}\right). \tag{23}$$

Table III gives C_{axial} as a function of "a".

Since, as explained for the solid wire case, the eddy current density vectors for circular and axial flux reversal are in quadrature,

$$s_w(\text{helical}) = \frac{s_w(\text{axial}) + s_w(\text{circular})}{2}. \tag{24}$$

Substitution of (21) and (23) into (24) gives the required expression;

$$s_w(\text{helical}) = \left(\frac{C_{\text{circ}} + C_{\text{axial}}}{2}\right)\frac{(B_s r_2^2)10^{-3}}{\rho_2\cos\theta}. \tag{25}$$

A number of composite wire samples have been prepared and evaluated. These include nickel on nichrome and nickel on copper. The switch-

TABLE III — THE PARAMETER "C_{axial}"

a	0.9	0.8	0.7	0.0 (Solid Wire)
C_{axial}	0.0795	0.300	0.633	3.142

ing curves for these samples as well as for a number of solid magnetic wires are shown in Fig. 9. The agreement between the measured values of s_w and the calculated values [(14) and (25)] is quite good. Improved composite wire samples are under development.

IV. EXPERIMENTAL MEMORY CELLS AND ARRAYS

The initial experiments were performed using commercially available nickel wire of 3-mil diameter. The φ-NI characteristic of this wire in the helical direction is extremely square. This is a feature of *all* the magnetic materials tested whether annealed or unannealed. As a typical example,

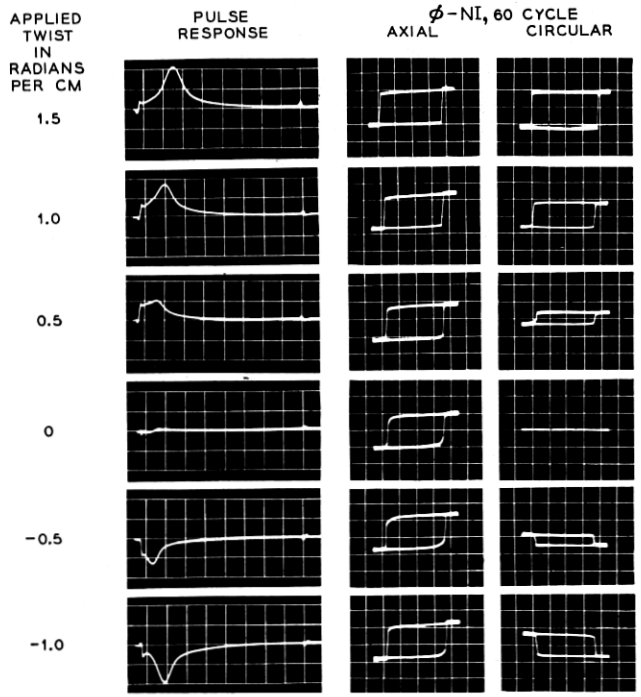

Fig. 11 — Sixty cycle and switching waveforms for 83 Ni, 17 Fe wire (see Fig. 9) as a function of applied torsion.

the 60-cycle characteristics of the axial and circular flux versus axial drive and the switching voltage waveforms under pulse conditions are given in Fig. 11 for 2-mil wire of composition 83 Ni, 17 Fe.

Note the negative prespike on the switching waveforms. By simultaneous observation of both the axial and circular switching voltage waveforms on many different magnetic wires it has been concluded that the negative prespike is due to an initial coherent rotation of the magnetization vector which results in an initial *increase* in the circular flux component. It is during this coherent rotation that the normal positive prespike on the axial switching voltage waveform is observed. Because of the mechanically introduced strain anisotropy, however, the magnetization vector is constrained to remain nearly parallel to the easy direction of magnetization. Thus, the coherent rotation soon ceases and the re-

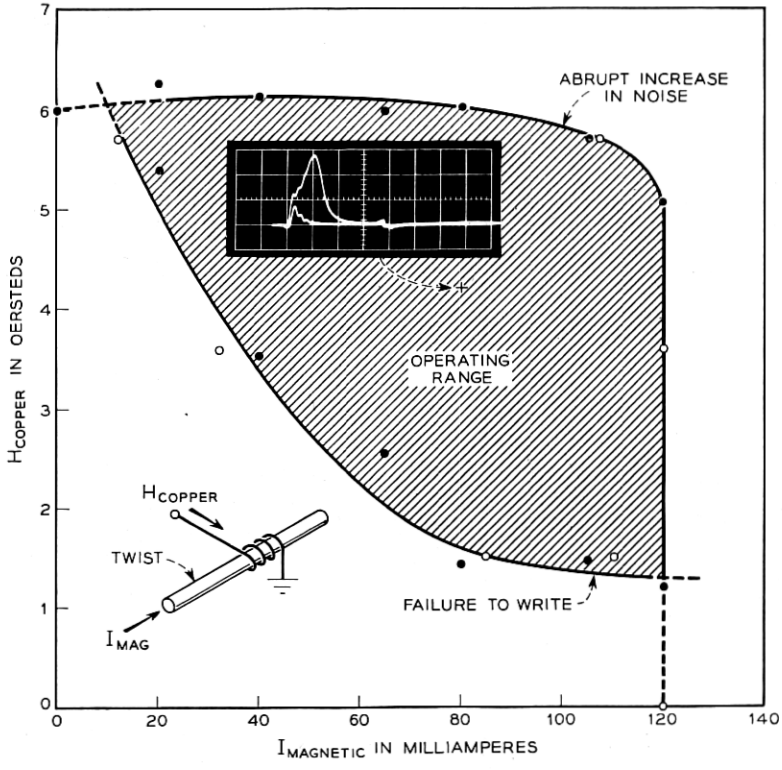

Fig. 12 — Range of writing currents for 83 Ni, 17 Fe wire operated mode. A Read drive held constant at 9 oersteds. Typical signal-to-noise ratio for a read is indicated.

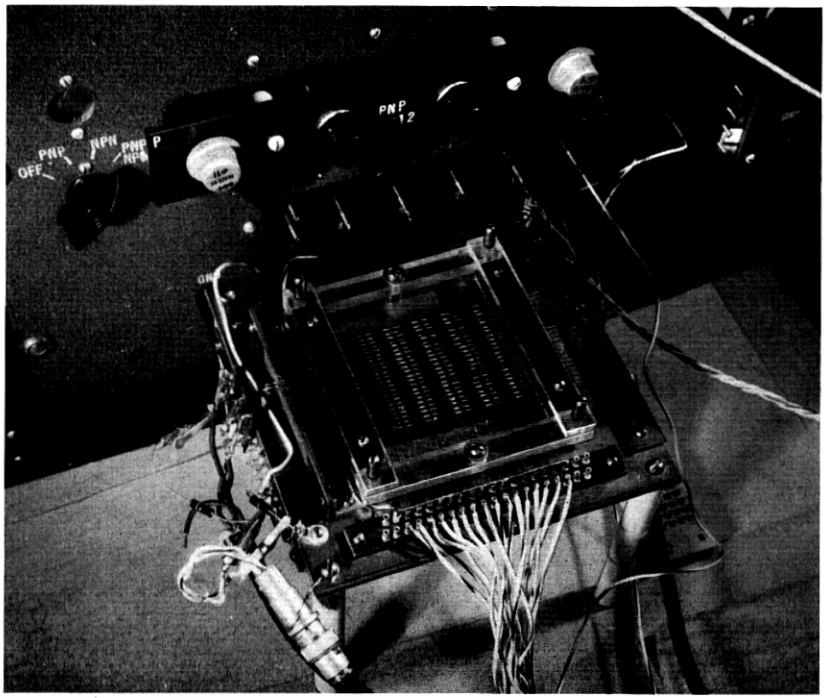

Fig. 13 — A 320-bit experimental twistor memory array. The array is transistor driven.

mainder of the flux reversal process is by an incoherent rotational process. During this latter time the circular and axial voltage waveforms are virtually identical.

Fig. 12 gives the range of operation of 2-mil 83 Ni, 17 Fe wire as a twistor operated by mode A. As a result of the extreme squareness of the φ-NI characteristic in helical direction the range of operation encloses an area nearly the theoretical maximum. The switching times of other memory cells tested ranged from 0.2 μsec for a 1 mil 4-79 moly-permalloy wire to 20 μsec for a 5 mil perminvar wire. Thus it is seen that the switching speeds of the twistor compare quite favorably with those of conventional ferrite toroids and sheets.

It is, of course, possible to store many bits of information along a single magnetic wire. The allowable number of bits per inch is related to the coercive force, the saturation flux density, and the diameter of the wire. For the nickel wire, about 10 bits per inch are possible. Predictions as to the storage density for a given material can be made by referring to

suitable demagnetization data. There are, however, interference effects between cells which are not completely understood at the present time.

A memory array (16 × 20) has been constructed as a test vehicle. An illustration of this array is shown in Fig. 13. The drive wires have been woven over glass tubes which house the removable magnetic wires. Provision is made for varying the torsion and the tension of the individual magnetic wires.

As an indication of the performance of the twistor, Fig. 14 is a composite photograph showing the minimum and maximum signal over the 16 bits of a given column for 3-mil nickel wire. Also included are the noise pulses for these cells, the so-called disturbed zero signals. The write currents were 2.3 ampere-turns on the solenoid and 130 ma through the magnetic wire. The read current was 6.0 ampere-turns. The array

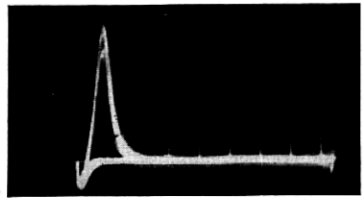

Fig. 14 — Composite photograph of the 16 output signals from a column of the array of Fig. 13. Average output signal about 3.5 millivolts; sweep speed equals 2 μsec/cm.

was transistor driven. A read-write cycle time of 10 microseconds appeared to be possible.

V. DISCUSSION

The twistor is presented as a logical companion to the coincident-current ferrite core and sheet.[6, 7] In many applications it should compete directly with its ferrite equivalents. Perhaps its greatest use will be found in very large ($>10^6$) memory arrays.

From a cost per bit viewpoint the future of the twistor appears quite promising. Fabricating and testing the wire should present no special problems as it is especially suited for rapid, automatic handling. The possibility of applying weaving techniques to the construction of a twistor matrix looks promising.

It is possible that, for both mode A and C operation of the twistor, an array can be built which consists simply of horizontal copper wires and

vertical magnetic wires — much like a window screen. Preliminary experiments have shown that single cross wires do operate successfully. The operation of this array would be analogous to a core memory array. Physically it could look just like a core array — but without the cores.

ACKNOWLEDGEMENTS

The author wishes to acknowledge the help of R. S. Title in obtaining the memory array data, R. A. Jensen in constructing the test jigs, and D. H. Wenny, Jr. in supplying the wire samples. The discussions with my associates, in particular D. H. Looney, R. S. Title, and J. A. Baldwin, have been very helpful. The writer would like to acknowledge the interest and encouragement shown by R. C. Fletcher.

APPENDIX I

From Fig. 10, for bulk circular flux reversal in a composite wire, the induced voltage $V(r)$ for a wire length l is

$$\begin{aligned} V(r) &= \left[(r_2 - r_1)l\left(\frac{2B_s}{T_s}\right)\right]10^{-8}, && 0 < r < r_1, \\ &= \left[(r_2 - r)l\left(\frac{2B_s}{T_s}\right)\right]10^{-8}, && r_1 < r < r_2. \end{aligned} \tag{26}$$

For a *solid* magnetic wire of radius r_2

$$V(0) = \left(\frac{2B_s r_2 l}{T_s}\right)10^{-8}. \tag{27}$$

Therefore,

$$\begin{aligned} V(r) &= \left(\frac{r_2 - r_1}{r_2}\right)V(0), && 0 < r < r_1, \\ V(r) &= \left(\frac{r_2 - r}{r_2}\right)V(0), && r_1 < r < r_2. \end{aligned} \tag{28}$$

In general, the resistance of a tube of wall thickness dr is $R(r) = \rho l/$

$2\pi r dr$. The resistance of the wire is $R_T = \rho_1\rho_2 l/\pi[\rho_1(r_2^2 - r_1^2) + \rho_2 r_1^2]$. The observable voltage for a length of wire, l, is

$$V_{\text{obs}} = \int [V(r)] \qquad \text{(Volt-Divider)}$$

$$= \int_0^{r_1} \left(\frac{r_2 - r_1}{r_2}\right) V(0) \left(\frac{\dfrac{\rho_1\rho_2 l}{\pi[\rho_1(r_2^2 - r_1^2) + \rho_2 r_1^2]}}{\dfrac{\rho_1 l}{2\pi r\, dr}} \right)$$

$$+ \int_{r_1}^{r_2} \left(\frac{r_2 - r}{r_2}\right) V(0) \left(\frac{\dfrac{\rho_1\rho_2 l}{\pi[\rho_1(r_2^2 - r_1^2) + \rho_2 r_1^2]}}{\dfrac{\rho_2 l}{2\pi r\, dr}} \right).$$

This reduces to

$$V_{\text{obs}} = V(0)\, \frac{(\frac{1}{3} - a^2 + \frac{2}{3}a^3)\rho_1/\rho_2 + a^2 - a^3}{(1 - a^2)\rho_1/\rho_2 + a^2} \tag{29}$$

$$= bV(0), \tag{30}$$

where $a = r_1/r_2$ and b is given by reference to (29). The ratio $b/\frac{1}{3} = 3b$ is the relative efficiency of the composite as compared to the solid magnetic wire from an available signal viewpoint. An expression for s_w will now be derived.

The total energy dissipated per unit length l is

$$\xi_T/l = T_s \int_0^{r_2} \rho i_d^2(r) 2\pi r\, dr, \tag{31}$$

where $i_d(r)$ is the current density. Now, $i_d(r) = V(r) - V_{\text{obs}}/\rho l$, therefore

$$\begin{aligned} i_d(r) &= (1 - a - b)\frac{V(0)}{\rho_1 l}, && 0 < r < r_1, \\ &= \left(1 - \frac{r}{r_2} - b\right)\frac{V(0)}{\rho_2 l} && r_1 < r < r_2. \end{aligned} \tag{32}$$

The substitution of (32) into (31) yields, after manipulations,

$$\xi_{\text{av}/l} = \frac{\pi T_s r_2^2}{\rho_2}\left(\frac{V(0)}{l}\right)^2 \left\{ a^2 \left[(1 - a - b)^2 \frac{\rho_2}{\rho_1} - (1 - b)^2 + \frac{4a(1 - b)}{3} - \frac{a^2}{2} \right] + (1 - b)^2 - \frac{4(1 - b)}{3} + \frac{1}{2} \right\}. \tag{33}$$

From (8), the applied energy per wire length l is

$$\xi/l = \left(\frac{[B_s(H - H_0)\cos\theta]10^{-7}}{2\pi}\right)\pi(r_2^2 - r_1^2), \tag{34}$$

where only that part of the applied energy associated with the high drive dynamic losses is included. Equating (33) and (34) and replacing $V(0)/l$ by (27) results in

$$s_w = (H - H_0)T_S = \frac{8\pi B_S r_2^2 10^{-3}}{\rho_2(1 - a^2)\cos\theta}\left\{a^2\left[(1 - a - b)^2\frac{\rho_2}{\rho_1} - (1 - b)^2 + \frac{4a(1 - b)}{3} - \frac{a^2}{2}\right] + (1 - b)^2 - \frac{4(1 - b)}{3} + \frac{1}{2}\right\}. \tag{35}$$

This can be expressed as

$$s_w = (H - H_0)T_s = C_{\text{circ}}\frac{(B_s r_2^2)10^{-3}}{\rho_2\cos\theta}\ (\text{oe-}\mu\text{sec}). \tag{36}$$

Bulk axial flux reversal in a composite magnetic wire can be treated in a manner analogous to that used in Section 3.1.1 for the solid wire. The uniform reversal of the axial flux induces a voltage $V(r)$ in the wire where

$$V(r) = V(r_2)\left[\left(\frac{r}{r_2}\right)^2 - \left(\frac{r_1}{r_2}\right)^2\right], \qquad r_1 < r < r_2,$$

$$= 0, \qquad 0 < r < r_1,$$

and $V(r_2) = [(2B_s/T_s)\pi r_2^2]10^{-8}$. Since $E(r) = V(r)/2\pi r$,

$$E(r) = \frac{B_S}{T_S}\left(r - \frac{r_1^2}{r}\right)10^{-8}. \tag{37}$$

Following the procedure of Section 3.1.1.,

$$\xi_{\text{av/cm}^3} = \frac{T_S 10^{-16}}{\pi(r_2^2 - r_1^2)}\int_{r_1}^{r_2}\frac{B_S^2}{\rho_2 T_S^2}\left(r - \frac{r_1^2}{r}\right)^2 2\pi r\, dr = \left\{\frac{2B_S^2 r_2^2 10^{-16}}{\rho_2 T_S}\left[\frac{\frac{1}{4} - a^2 + a^4(\frac{3}{4} - \ln a)}{1 - a^2}\right]\right\}, \tag{38}$$

where $a = r_1/r_2$ as before. Equating this expression to (8) yields

$$s_w = (H - H_0)T_S = \frac{\pi B_S r_2^2 10^{-3}}{\rho_2\cos\theta}\left[\frac{1 - 4a^2 + a^4(3 - 4\ln a)}{1 - a^2}\right] \tag{39}$$

$$= C_{\text{axial}}\left(\frac{B_S r_2^2 10^{-3}}{\rho_2\cos\theta}\right)(\text{oe-}\mu\text{sec}). \tag{40}$$

REFERENCES

1. R. M. Bozorth, *Ferromagnetism*, D. Van Nostrand Company, Inc., New York, N. Y., 1951, p. 628.
2. U. F. Gianola, Use of Wiedemann Effect for Magnetostrictive Coupling of Crossed Coils, T. Appl. Phys., **26,** Sept. 1955, pp. 1152–1157.
3. H. F. Girvin, *Strength of Materials*, International Textbook Co., Scranton, Pa., 1944, p. 233.
4. J. A. Baldwin, unpublished report.
5. H. J. Williams, W. Shockley, and C. Kittel, Velocity of a Ferromagnetic Domain Boundary, Phys. Rev., **80,** Dec. 1950, pp. 1090–1094.
6. J. A. Rajchman, Ferrite Apertured Plate for Random Access Memory, Proc. I.R.E., **45,** (March, 1957), pp. 325–334.
7. R. H. Meinken, A Memory Array in a Sheet of Ferrite, presented at Conference on Magnetism and Magnetic Materials, Boston, Mass., Oct. 16–18, 1956.